Tomasz WĘGLIŃSKI
Anna FABIJAŃSKA

THE CONCEPT OF IMAGE PROCESSING ALGORITHMS FOR ASSESSMENT AND DIAGNOSIS OF HYDROCEPHALUS IN CHILDREN

ABSTRACT *This paper presents a concept of image processing and analysis algorithms for an automatic assessment of hydrocephalus in children's brain. Presented research was inspired by the medical need for tools performing an automatic (or at least semi-automatic) detection and quantitative evaluation of this lesion. Algorithms for precise segmentation of hydrocephalus and determination of its volume from three dimensional CT brain scans were introduced. Specifically, for brain and hydrocephalus segmentation, region growing approach was proposed. Results of applying the developed method to real CT data sets were presented and discussed. The analysis of the results show that in future, the proposed algorithms can be helpful tool for diagnosis of hydrocephalus.*

Keywords: *hydrocephalus, CT, image segmentation, region growing.*

Tomasz WĘGLIŃSKI, M.Sc.
e-mail: tweglinski@kis.p.lodz.pl

Anna FABIJAŃSKA, Ph.D.
e-mail: an_fab@kis.p.lodz.pl

Computer Engineering Department
Technical University of Lodz

PROCEEDINGS OF ELECTROTECHNICAL INSTITUTE, Issue 251, 2011

1. INTRODUCTION

Medical imaging is a group of examinations, techniques and processes that use different types of physical effects to visualize anatomical structures and pathological changes inside the human body [1]. Recently, it is one of the fastest growing fields of medical examinations. Development of medical imaging techniques contributed to a significant increase in the effectiveness of detection and treatment of various lesions and pathological changes.

Radiological examinations allow for an accurate detection of the lesion. Proper analysis of the disease is crucial to make decision of the treatment. However, manual assessment of pathological changes is always subjective and time-consuming. There is also a risk that such assessment can be cursory and incorrect. Therefore, development of tools for an automatic detection and analysis of pathological changes is one of the most challenging tasks of a present day medical image processing and analysis.

Recent studies in medical image processing follow in many directions. There are researches focused on the segmentation of abdomen [2, 3], heart [4, 5], lung [6, 7], brain [8-10] etc. In this paper, attention is paid to the problem of detection and analysis of a common disease that affects the human brain, called hydrocephalus.

Hydrocephalus is the most common disease of the central nervous system in children and require neurosurgical treatment. Although this condition may appear in a patient at any age, most often it affects newborns and infants in the first year of life. It is estimated that hydrocephalus occurs in approximately one in 500 newborns. More than half a of surgical interventions performed in this period of life is carried out for this reason. In the scale of a country like Poland it is more than a 1000 operations a year [11].

Hydrocephalus has been studied and imaged for many years however, there is no common solution and effective method for precise detection and quantitative assessment of this lesion. Existing measurement methods are mostly qualitative and do not give satisfactory results. Therefore, the use of image processing techniques combined with mathematical analysis of the key characteristics (like size and volume of the lesion) may be an important step forward to improvement of hydrocephalus diagnosis reliability. This paper shows the concept of using image processing algorithms to support the diagnosis of hydrocephalus in children.

The following part of this paper is organised as follows. Firstly, in Section 2 some basic medical background on hydrocephalus is given. Next, in Section 3 researches related to application of image processing methods for

assessment of hydrocephalus are briefly reviewed. This is followed in Section 4 by description of image data used in this work. The proposed method is described in detail in Section 5. Preliminary results provided by the proposed approach are presented and discussed in Section 6. Finally, Section 7 concludes the paper.

2. MEDICAL BACKGROUND

The central nervous system consists of two interconnected parts: the cerebrum located within the cranial cavity and spinal cord located in the middle of the spine. The cerebrum consists of three structures: the brain, cerebellum and brain stem. Inside the cerebrum there is normally a small space filled with cerebrospinal fluid chamber called ventricular system of the brain. Figure 1 shows the general structure of the brain. Ventricular system is marked with blue colour.

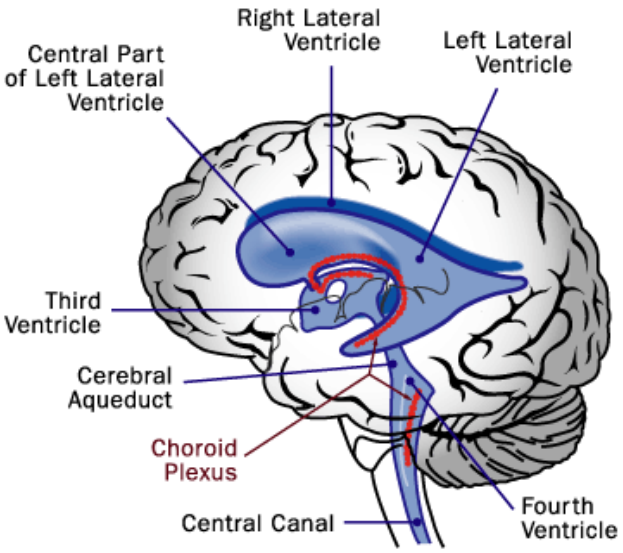

Fig. 1. The general structure of the brain with ventricular system marked blue [12]

Hydrocephalus (also known as "water on the brain") is a pathological condition in which the effect of dynamic circulatory disorders of the cerebrospinal fluid (CSF) comes to their excessive accumulation in the intracranial space and results in the increase of intracranial pressure. Hydrocephalus is caused by upset of the natural balance between production, flow and absorption of CSF, which accumulates mostly around the ventricular system, causing it to expand [11]. Figure 2 shows the comparison between ventricular system of the healthy brain and brain affected by hydrocephalus.

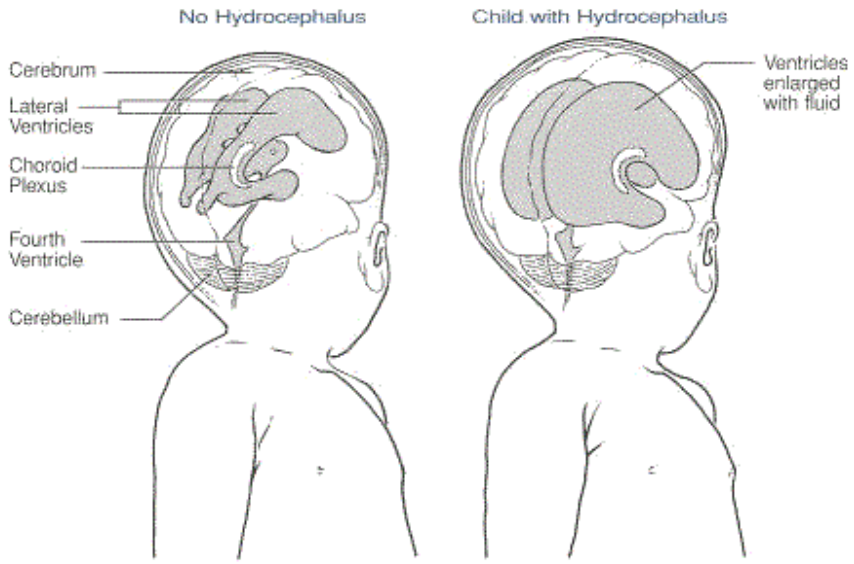

Fig. 2. Ventricular system of the healthy brain and affected by hydrocephalus [13]

Clinical symptoms of elevated intracranial pressure is an indication for brain imaging. Among the radiological methods that assess the anatomical structures of the central nervous system and circulation of cerebrospinal fluid are: ultrasonography (USG), computed tomography (CT) and magnetic resonance imaging (MRI). CT and MRI scanners produce digital images in DICOM format, which can be easily processed.

Present day CT and MRI scanners produce digital images, which can be easily stored and processed. Recently used devices produce high-quality grayscale images, coded in 12 or 16 bits of signed or unsigned short values. One examination produces about 15±20 images in case of CT and 25±100 for MRI study. Each image corresponds to the consecutive cross-section of the brain. The spatial resolution of a single cross section vary depending on imaging device from 256×256 to 1024×1024 pixels. Such examination usually covers only some part of the brain, most interesting from the standpoint of the disease. Consecutive images (cross sections) are always in constant distance from each other. This distance is determined by the radiologist before the examination and is called *slice thickness*. The highest the distance, the less number of images is produced. As a result, more information about the brain must be reconstructed. Figure 3 shows the general schema of the CT examination with exemplary lower bound marked green.

Pathological change in brain tissue due to hydrocephalus is often clearly visible in the CT images. This lesion is characterized by a significant widening of brain ventricular system where the cerebrospinal fluid is accumulated.

Additionally, in CT images, the intensity of hydrocephalus is significantly darker than the intensities of healthy brain, so the lesion can be easily distinguished.

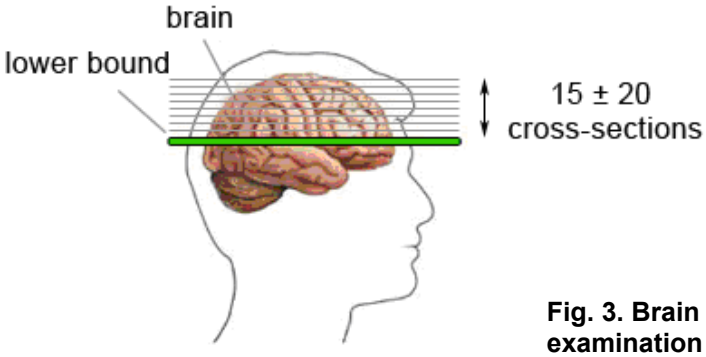

Fig. 3. Brain area significant for CT examination

Figure 4 presents the comparison between cross sections from the CT scan of a healthy brain (Fig. 4a) and a brain affected by the hydrocephalus (Fig. 4b). The border of a brain tissue is outlined by green line. Borders of brain region affected by hydrocephalus are marked with red line.

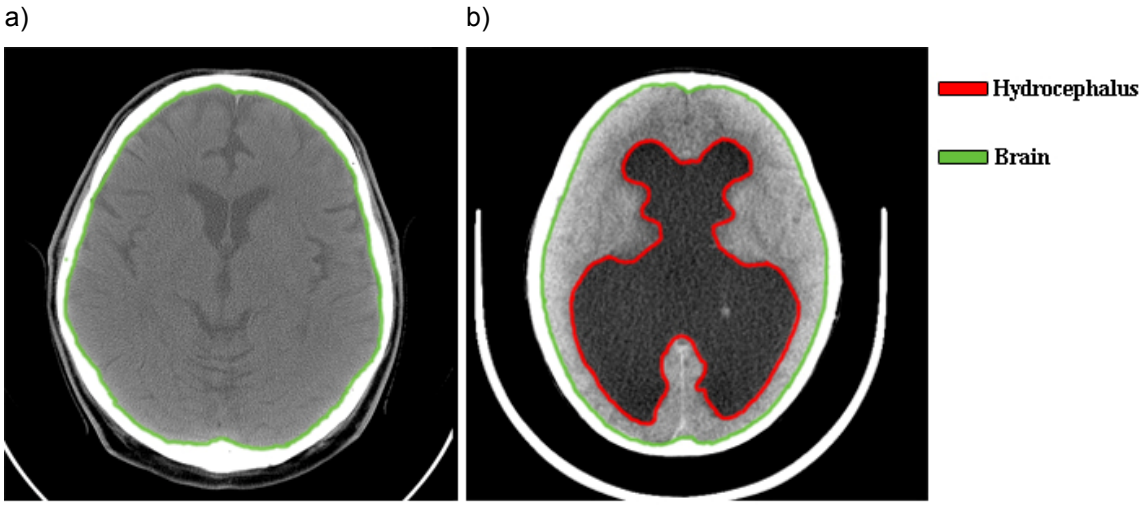

Fig. 4. Exemplary CT cross sections of brain:
a) healthy brain; b) brain affected by the hydrocephalus

It must be remembered that not every brain ventricular enlargement is caused by hydrocephalus and requires surgical treatment. Therefore, in order to decide if the disease process is active, it is necessary to calculate the appropriate parameters.

For many years, the abnormal width of the ventricular system was assessed by means of the Evans' ratio. It is an encephalographic ratio for estimating ventricular enlargement and cerebral atrophy. The ratio is calculated by

the division of the transverse diameter of the anterior horns of the lateral ventricles to the internal diameter of the skull. It is believed that the disease process is active for ratios above 0,3 (30%) [14].

Figure 5 presents the CT brain scan with lines indicating diameters used for calculation of Evan's ratio. Specifically, diameter A denotes anterior horns of the lateral ventricles and diameter B is the greatest internal diameter of the skull.

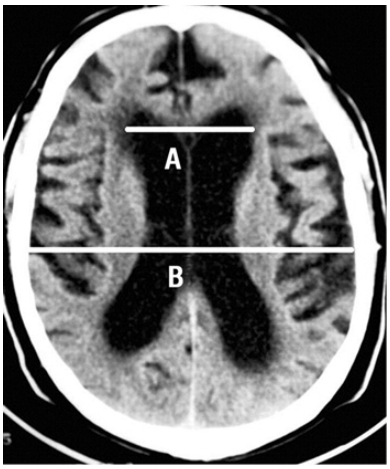

Fig. 5. Lines indicating diameters used for calculation of Evan's ratio from CT brain scan:
A – anterior horns of the lateral ventricles, B – greatest internal diameter of the skull

However, assessment of hydrocephalus progress using Evans' ratio is often tentative, therefore recently, medicine is looking for a new – more reliable and competent solutions and measures dedicated for assessment of hydrocephalus progress [11]. It is believed [15, 16] that a better solution would be to calculate the ratio between the volume of the lesion to the volume of the whole brain. However, such calculation cannot be performed manually, because it is too cumbersome and too time-consuming for everyday clinical routine. Therefore, there is a need to automate this process. This fact was an inspiration for the research presented in this paper.

3. RELATED WORKS

Due to the complexity and large variations of anatomical structures of human brain, problem of the detection and analysis of the brain diseases is a challenging task for recent medical image processing. However, although a plenty of methods for the segmentation of brain ventricular system have already been proposed [17-19], algorithms for detection and quantitative assessment of the hydrocephalus are still under development and only several approaches have been reported [20-23, 25] so far. These are briefly characterized below.

The objective of the research performed by Kobashi et al. [23] was to introduce a computer-aided diagnosis system (CAD) which is mainly able to segment the cerebrospinal fluid (CSF) and the lateral ventricles from MRI

images. The developed software may also calculate the volumes of segmented areas. The developed method was based on a 3D region growing algorithm and fuzzy inference techniques. It was tested on 60 patients including 20 with indicated hydrocephalus. The qualitative evaluation by a physician showed that developed method gives good results but the segmentation algorithm has an noticeable error which may disrupt the volume calculations.

Research performed by Pustkova et al. [20] was aimed at the development of semi-automatic method for segmentation of ventricular system from volumetric CT and MRI brain scans. Their method was developed in order to perform volume measurements of the intracranial fluids. Calculation of the CSF volume before and after surgery may show whether the treatment process was successful. However, method proposed in [20] involves the manual selection of the CSF area from single images and has a significant 10% error in segmentation precision.

Sweetman et al. [24] considered the problem of computational prediction of cerebrospinal fluid flow in human brain. By the use of image reconstruction software Mimics 12.11, the authors developed the 3D model from MRI brain images, which reproduces pulsatile CSF motion and predicts intracranial pressures and flowrates. The model of a healthy brain helps to predict CSF flow correctly, however accurate prediction of pathological brain dynamics (such as hydrocephalus) require model refinement.

The objective of the research performed by Butman and Linguraru [21] was to develop an algorithm for the assessment of ventricle volume from MRI brain scans in communicating hydrocephalus. Proposed approach uses a combination of fast marching and geodesic active contour level sets to segment the enlarged ventricular system. The results of the segmentation allows to perform volume calculations, however the disadvantage of this technique is computational overhead, so such solution cannot be applied in everyday clinical use.

Halberstadt and Douglas [25] used fuzzy clustering technique to segment CT brain images with indicated hydrocephalus. Algorithm was developed to perform further calculations of the ventricle/brain ratio (VBR). The VBR is calculated by dividing the number of pixels in the ventricle area by the number of pixels in the brain area. However, after segmentation process, user have to manually (using mouse) label the regions by selecting each ventricle region, as well as the brain region, which seems to be very cumbersome requirement.

Research performed by Ambarki, et al. [22] was aimed at testing and evaluating the existing automatic tool for brain segmentation and analysis called Qbrain. Tests were performed on 20 datasets from MRI examinations of patients with indicated hydrocephalus. Qbrain is able to detect hydrocephalus area from the images and calculate its volume. Obtained results can be compared with currently known measurement methods. However, Qbrain

segmentation algorithm still need to be improved, so the calculated volume is often inaccurate.

Study of the literature concerning application of image processing and analysis for hydrocephalus assessment and diagnosis shows that most of already performed researches are generally new. Developed methods for detection and quantitative assessment of this lesion still need to be improved and substantial work in this field is still to be done.

4. INPUT DATA

In this research, several image volumetric datasets from computer tomography brain examinations were used. Each dataset corresponded to one examination. In order to verify the universality of proposed methods, it was decided to select examinations of few children at a different stages of their life. A difficulty was that the selected datasets were provided by different CT scanners and in consequence were characterized by different properties. Specifically, there were significant differences in intensity range used for depicting brain information.

Single cross sections from exemplary CT datasets used in the described research are presented in Figure 6. The examinations were numbered from 1 to 8. For further reference the number of the examination is indicated in subfigure caption.

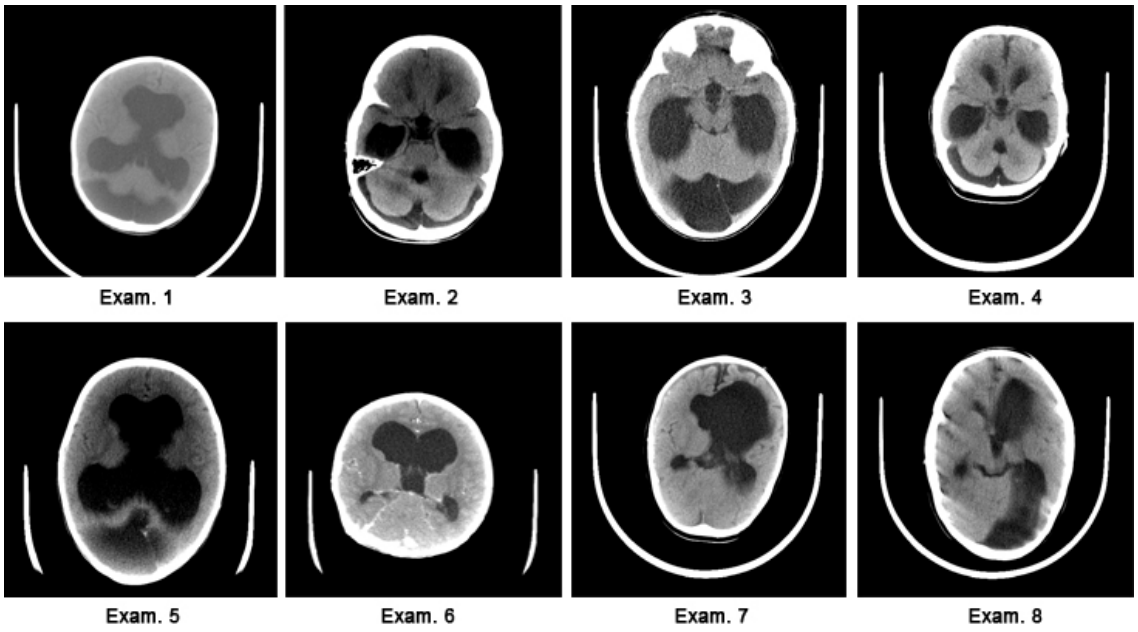

Fig. 6. Single images from the CT datasets used in this research

All datasets regarded in this research consisted of about 15±20 gray-scale images (representing consecutive cross section of brain) stored in DICOM format. Images were coded on 16-bit signed or unsigned short integer values. Spatial resolution of every image was 512×512 pixels.

One of the most important feature of the DICOM format is the information stored in header of each file. The header contains significant information about manufacturer of the scanner, type of the study, the patient's position and distance from the imaging device, the detailed properties of produced images, etc. For the methods proposed in this research, several parameters from DICOM header were especially important. Table 1 shows variables from the DICOM header used in this research, with their short description.

TABLE 1
Selected parameters from DICOM header used in this work [26]

Variable code (group, element)	Variable name	Description
(0028,1052)	Rescale intercept	The value b in relationship between stored values (SV) and the output units. Output units = m* SV + b
(0028,1053)	Rescale slope	The variable m in the equation specified by rescale intercept (0028,1052)
(0028,1050)	Window center	The variable describing the brightness of the image
(0028,1051)	Window width	The variable describing the contrast of the image
(0028,0030)	Pixel spacing (X, Y)	The spacing between pixels in the image (mm)
(0018,0050)	Slice thickness	The spacing between consecutive cross sections (mm)

5. METHODS AND PRELIMINARY RESULTS

The main objective of the described research was to develop image processing methods for an automatic determination of hydrocephalus volume and its relation to the volume of the whole brain.

The calculation of ratio between these two volumes (i.e. volume of pathological change due to hydrocephalus and volume of brain) requires two main steps which are as follows:

- extraction of the brain from consecutive CT images;
- the extraction of the pathological change caused by hydrocephalus from consecutive CT images.

Then, the approximate ratio may be calculated regarding the number of pixels qualified to each region.

This paper proposes several image processing methods which may be the basis for the automatic detection of hydrocephalus in children. Then, the approximate ratio between the volume of the brain and the volume of hydrocephalus is calculated. Presented solution works in three stages which are as follows:

1. segmentation of the intracranial brain area;
2. segmentation of hydrocephalus;
3. calculation of the brain and hydrocephalus volumes.

The above mentioned steps are described in details in the following subsections.

5.1. Segmentation of the intracranial brain area

The first step of the proposed method is segmentation of the intracranial brain area. This step consist of three stages, which are as follows:

- image enhancement;
- skull removal;
- brain extraction.

Image enhancement

The images used in this research were obtained from different CT scanners and are characterised by different ranges of intensities. Therefore, before the main image processing algorithms are applied, input images must be enhanced by normalizing intensities of all input cross section to a common range.

It was decided to transform image intensities to unsigned short values, coded in 12 bits. The resulting range of intensities from 0 to 4095 fully cover the Hounsfield scale. Conversion is performed according to the recommendations given in DICOM specification [10]. According to the DICOM specification, every pixel in the image is scaled in accordance to the following formula:

$$g(x,y) = f(x,y) \cdot R_s + R_i \tag{1}$$

where:

$g(\cdot)$ – output intensity,
$f(\cdot)$ – input intensity,
R_s – rescale slope (see Table 1),
R_i – rescale intercept (see Table 1),
x, y – pixel coordinates.

After scaling image intensities to a common range, with the use of other DICOM header information (such as *window width* and *window center*) pixel intensities are transformed from signed to unsigned values without any changes in image quality. Operation applied in this is described by Equation (2).

$$g'(x,y)=\begin{cases} g_{\min} \ \ for\ g(x,y)\le a \\ g_{\max} \ \ for\ g(x,y)>b \\ h(x,y) \ \ for\ a<g(x,y)\le b \end{cases} \tag{2}$$

where:

$$a = c - 0.5\cdot(2-w) \tag{3}$$

$$b = c - 0.5\cdot w \tag{4}$$

$$h(x,y)=\frac{g(x,y)-(c-0.5)}{(w-1)+0.5}\cdot(g_{\max}-g_{\min})+g_{\min} \tag{5}$$

and:

$g'(\cdot)$ – input pixel intensity,
$g(\cdot)$ – output pixel intensity,
g_{min} – requested minimum output intensity,
g_{max} – requested maximum output intensity,
w – window width (see Table 1),
c – window center (see Table 1).

The values of g_{min} and g_{max} are set to 0 and 4095 respectively.

Results of intensity transformation applied to exemplary image are presented in Figure 7. Specifically, Figure 7a presents original image and Figure 7b presents image after preprocessing.

a) b) c)

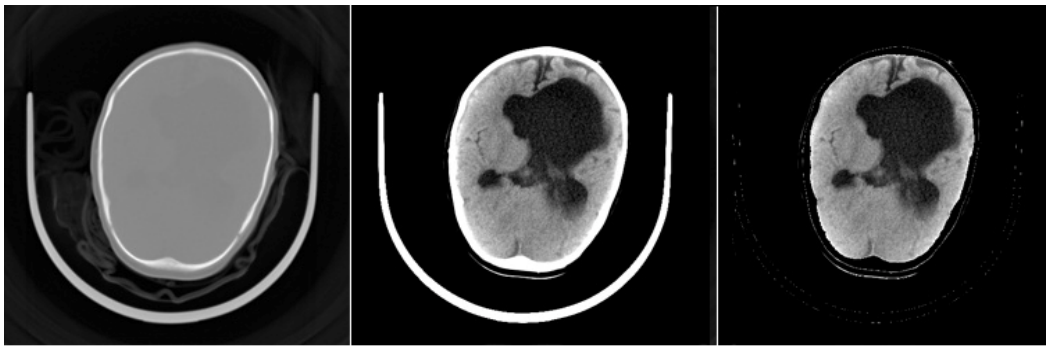

Fig. 7. Successive steps of segmentation of the intracranial brain area;
a) original image; b) image after intensity transformation; c) results of skull removal

Skull removal

Conversion of image intensities carried out in the first step emphasizes skull information. Pixel intensities that were above the value specified by Equation (4) received the highest intensity value in 12 bit range – 4095. This value is used as a threshold. As a result, the skull area can be then accurately removed from input images. Furthermore, the result of thresholding shows that also fragments of the CT machine tube, visible in every image, was successfully removed.

Results of thresholding applied to exemplary image from Figure 7b are presented in Figure 7c. It can be easily observed, that skull and other redundant information was successfully removed from the analysed image.

Brain extraction

In the last step brain region is extracted. For this purpose, the 2D segmentation algorithm is applied to consecutive images from the dataset. The method is seeded region growing approach. The seed point is located at the center of the each cross section, as this point always belongs to the brain. Starting from this seed, the consecutive pixels are tested for the similarity to the desired area. Only pixels of certain properties are joined to the region.

Due to properties of the analysed images brain region can be easily extracted. Specifically, the condition for adding the next pixel to the brain region is that the intensity of candidate pixel must be over 0 (as this intensity always belongs to background). Otherwise, such pixel is treated as background.

The schema of an algorithm for brain extraction is presented in Figure 8.

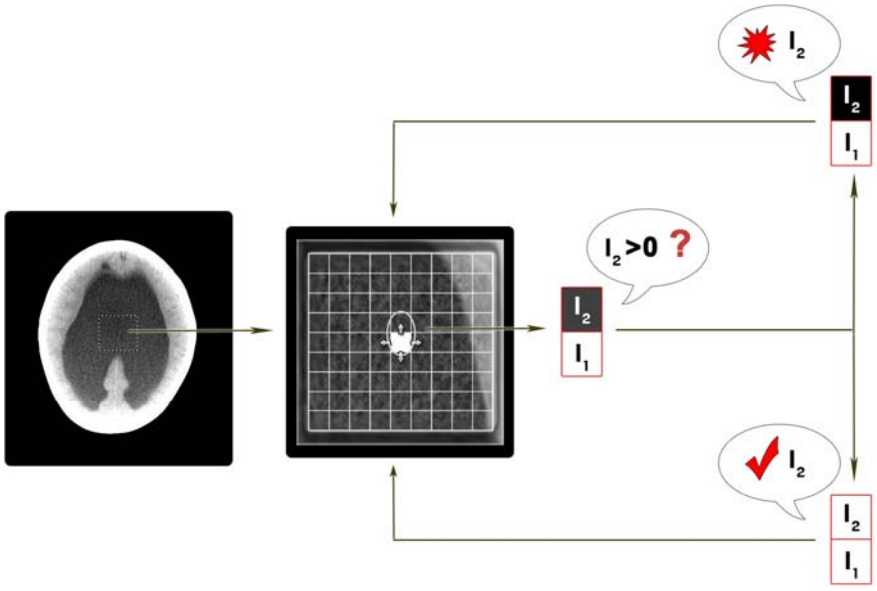

Fig. 8. Scheme of brain extraction algorithm based on seeded region growing

The results of applying the proposed algorithm to several cross sections from exemplary dataset are presented in Figure 9.

a)

b)

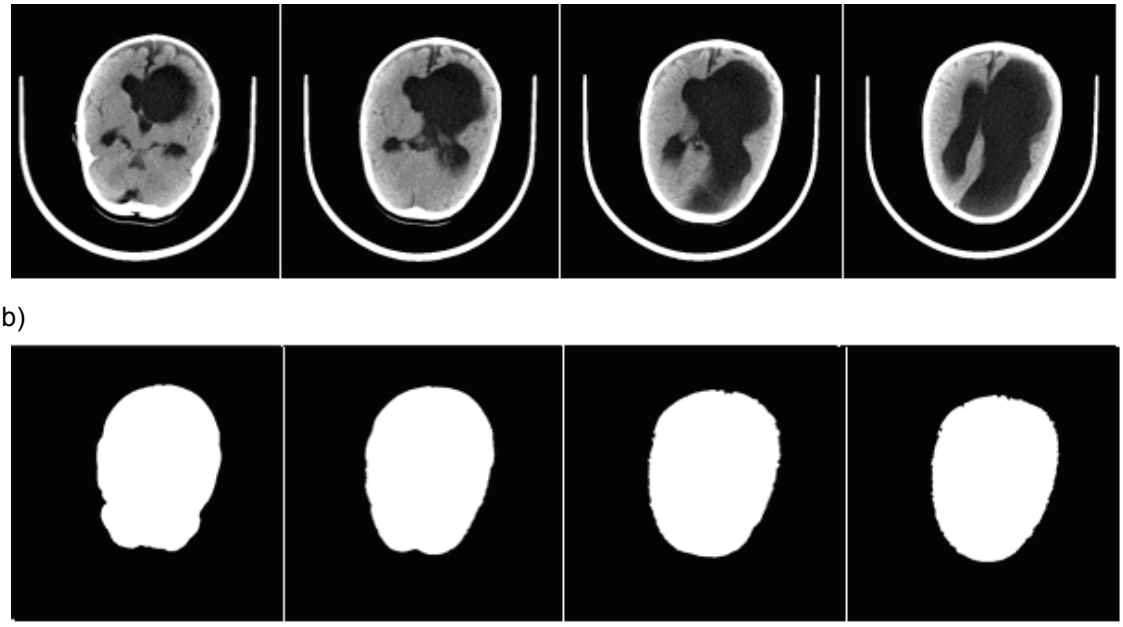

Fig. 9. Results of applying brain extraction algorithm to exemplary brain images: a) original images, b) brain segmentation

5.2. Segmentation of hydrocephalus

The second step of the proposed method aims at extraction of hydrocephalus. For this purpose, firstly several popular thresholding algorithms were applied. Specifically, the following methods were regarded:

1. IsoData [27];
2. Moments [28];
3. Max Entropy [29].

Thresholding methods applied for each 2D image, segment all the CSF visible in cross sections. The results of applying thresholding methods were presented and discussed in previous paper [30]. This work showed that the MaxEntropy algorithm gives subjectively the best results, presented in Figure 10.

Results provided by the traditional thresholding approaches do not provide satisfactory results. In binary images presented in Figure 10 it can be seen that some information about brain change due to hydrocephalus is lost. Therefore, in order to perform segmentation more accurately, 2D seeded region growing approach was used again for lesion segmentation. Specifically, method

applied previously for brain segmentation was modified. The main improvement of this method is a selection of starting seed points (SSP). For hydrocephalus segmentation seed points are selected based on histograms of consecutive CT brain cross sections.

a)

b)

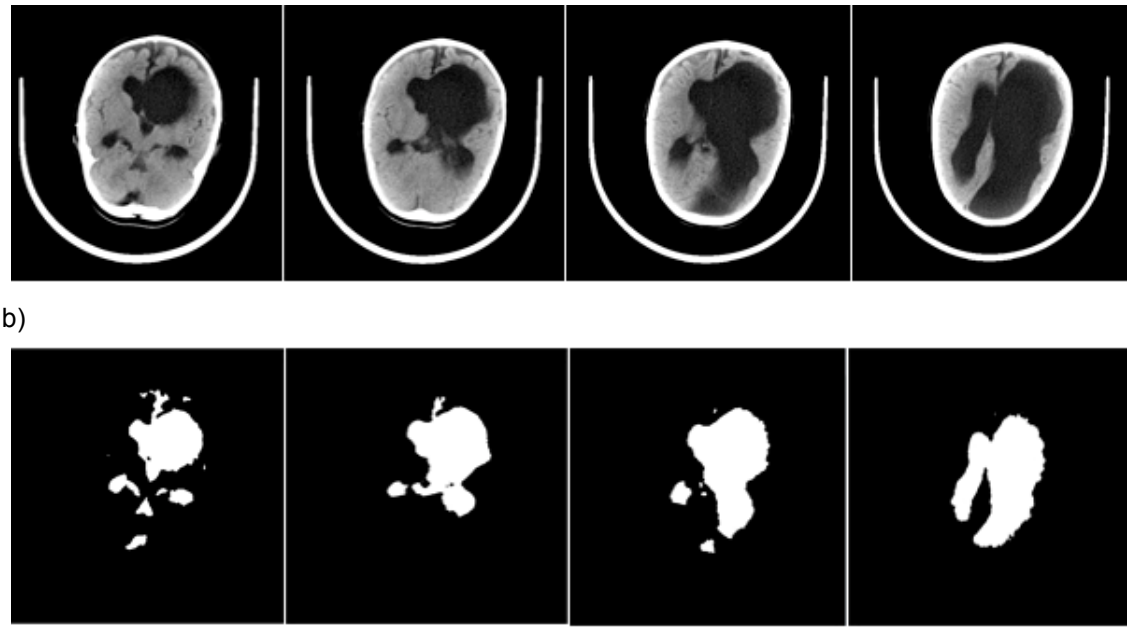

Fig. 10. Results of MaxEntropy thresholding applied to CT images from exemplary dataset: a) original images, b) hydrocephalus segmentation

In Figure 11 histograms of exemplary CT brain images are shown. They correspond with cross sections from examinations 1-4 shown in Figure 6 and were obtained after brain extraction (see. Sect. 5.1). Specifically, intensities located in background area, skull and bolster region were excluded from histogram calculation.

It can be easily seen that presented histograms have very similar shape as they are strongly bimodal. It can be also seen from Figure 11 that there are three characteristic elevations of pixel intensities in the image histograms. First rise (at 0) belongs to background. Second rise, with lower intensity values, belongs to pathological change due to hydrocephalus. Finally, the third elevation belongs to brain area. The algorithm for SSP selection was designed to separate histogram peaks by finding floor of the histogram valley, i.e. the point (intensity) where the histogram function changes from decreasing to increasing. The algorithm ignores zero intensity, which is not regarded as a region. Figure 12 presents the exemplary image histogram with marked areas belonging to hydrocephalus and brain.

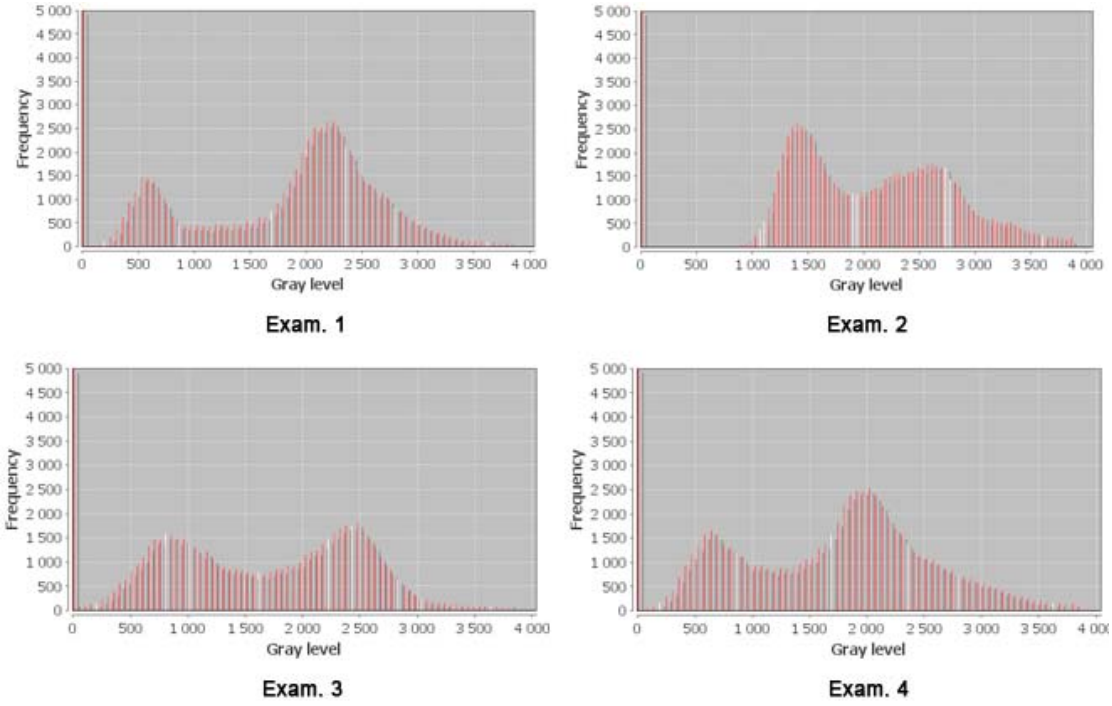

Fig. 11. Histograms of exemplary images obtained from images after brain extraction

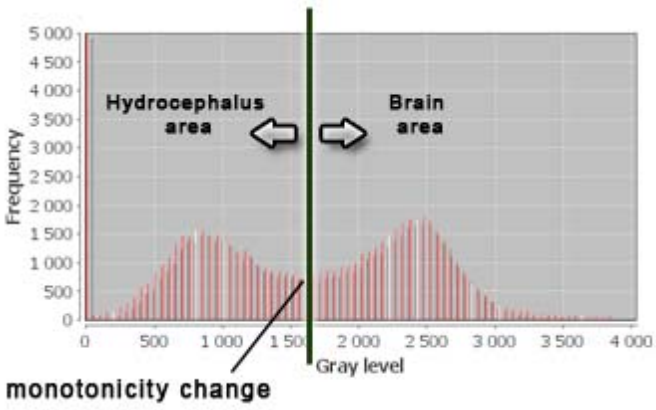

Fig. 12. Exemplary histogram with marked areas of hydrocephalus and brain

After selecting the intensities belonging to each region, the algorithm for finding SSP determines 5 maximal intensity values from the lesion area. These values correspond to the image pixels which have the highest probability to belong to the desired region hence they indicate possible seeds for region growing. Therefore, the algorithm randomly selects at least 50 pixels of these in-tensities in order to perform further statistical calculations.

Specifically, points (pixels in the image) selected by the SSP algorithm are the initial seeds for the developed 2D segmentation algorithm based on region growing. It was tested that pixel intensity values are normally distributed. Thus, in accordance with the *three sigma* rule [Eq. (6)], region intensity values I can differ from its expectation $\bar{x}$ by a quantity exceeding 3σ on the average in not more than 3 times in a thousand trials [31].

$$P\left\{\bar{x} - 3\sigma \le I \le \bar{x} + 3\sigma\right\} = 0.99730 \tag{6}$$

where σ denotes standard deviation of intensities.

Equation 6 defines the scope of permissible difference between the starting seed point and the next candidate pixel. If this condition is fulfilled, new pixel is joined with the region. Added pixel is also marked as the next seed point. Figure 13 shows the complete diagram of the described 2D segmentation algorithm.

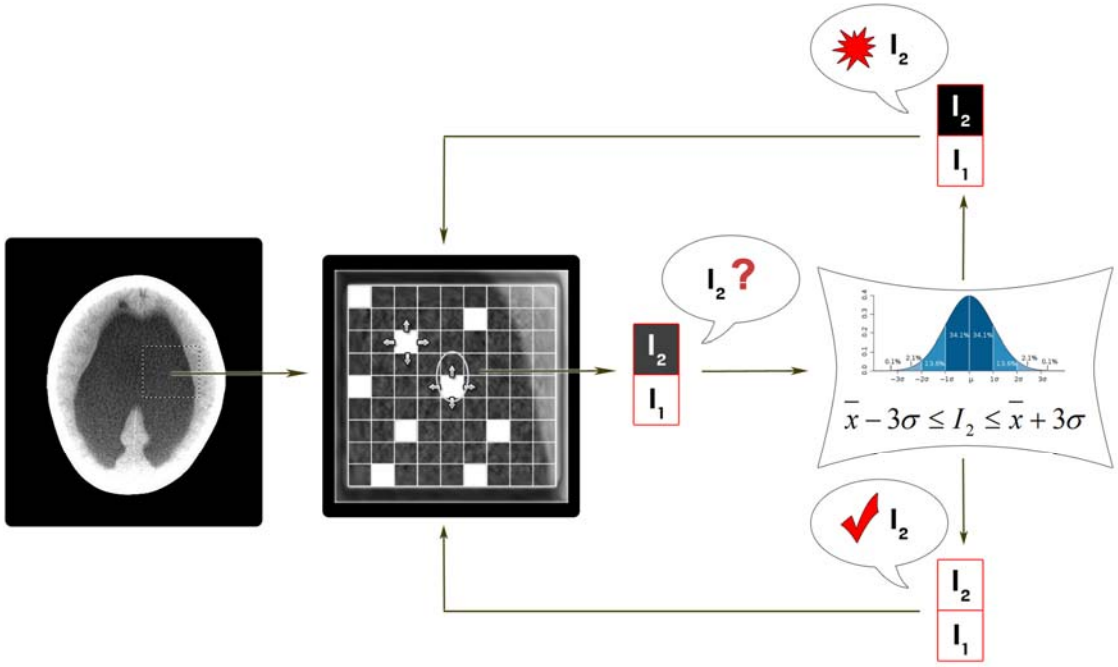

Fig. 13. Diagram of the developed 2D hydrocephalus segmentation algorithm based on seeded region growing

Results of applying the proposed 2D segmentation algorithm to several CT brain cross sections from exemplary dataset are presented in Figure 14. Original images are shown in Figure 7.

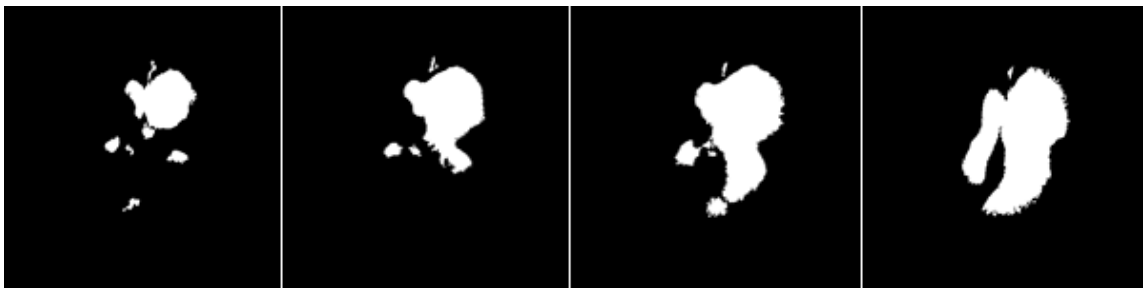

Fig. 14. Results of hydrocephalus segmentation using the proposed 2D region growing approach. Original images are shown in Figure 10

5.3. Determination of brain and hydrocephalus volumes

The final stage of the proposed approach is aimed at the calculation of volumes of brain, hydrocephalus and a ratio between them (referred as H/B ratio). These both volumes can be easily calculated directly from binary images of the corresponding regions obtained in the previous steps of image processing.

In case of the considered volumetric images single pixel can be regarded as cuboid of height equal to *slice thickness* and base of dimensions equal to *pixel spacing* X and *pixel spacing* Y respectively (see Figure 15). Hence, the volume V_p of single pixel is described by Equation (7).

$$V_p = d \cdot s_x \cdot s_y \tag{7}$$

where:

d – slice thickness,
s_x – pixel spacing X,
s_y – pixel spacing Y.

All these parameters are stored in a header of DICOM files (see Table 1).

Having volume of a single pixel, an approximate volumes of brain and hydrocephalus can be easily calculated simply by counting number of pixels qualified (by segmentation algorithms) to these regions and multiplying the result by a volume of a single pixel in accordance with Equations (8) and (9). It should be underlined, that all CT brain cross sections from the dataset should be regarded in this step. This idea sketched in Figure 15.

$$B = V_p \sum_{z=1}^{n} \sum_{x=1}^{M} \sum_{y=1}^{N} b(x, y, z) \tag{8}$$

$$H = V_p \sum_{z=1}^{n} \sum_{x=1}^{M} \sum_{y=1}^{N} h(x, y, z) \tag{9}$$

where:

B – volume of brain,
H – volume of hydrocephalus,
n – number of images (brain cross sections) in the dataset,
M, N – dimensions of a single cross section (in pixels),
b – binary image of brain,
h – binary image of hydrocephalus.
x, y, z – pixel coordinates.

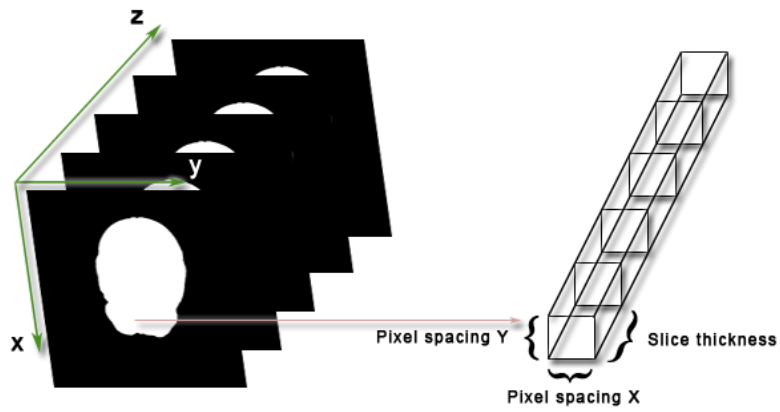

Fig. 15. The idea of brain volume calculation from binary images

Having approximate volumes of brain and hydrocephalus ratio between them can be easily calculated using the following equation.

$$R_{H/B} = 100\% \frac{H}{B} \tag{10}$$

6. PRELIMINARY RESULTS AND DISCUSSION

In this section numerical and visual results of applying the proposed method to exemplary CT brain scans are given.

Numerical results obtained for 8 exemplary CT examinations (shown in Figure 6) are presented in Table 2. Specifically, in the first column number of examination is indicated. In the second and the third column the determined volumes of brain and hydrocephalus are given (in mm^3). Finally, the last column contains an information about H/B ratio determined for a given examination.

TABLE 2
Volumes of hydrocephalus and brain determined for exemplary CT datasets

No. of exam.	Brain (B) vol. [mm^3]	Hydrocephalus (H) vol. [mm^3]	Ratio H/B [%]
1.	1194723.63	402297.36	33.67
2.	1115397.95	436798.83	39.16
3.	431212.28	123166.23	28.56
4.	998670.41	364546.14	36.5
5.	1033167.48	278540.77	26.96
6.	1119629.88	433302.98	38.7
7.	823233.03	247335.21	30.04
8.	1310280.03	452124.76	34.51

The 3D visualization of brain and pathological change due to hydrocephalus for two exemplary examinations are shown in Figures 16 and 17. Specifically, in Figure 16 results obtained for examination no. 1 are shown, while Figure 17 corresponds with examination no. 4. In case of both figures brain area is presented in subfigure (a) while subfigure (b) presents the lesion.

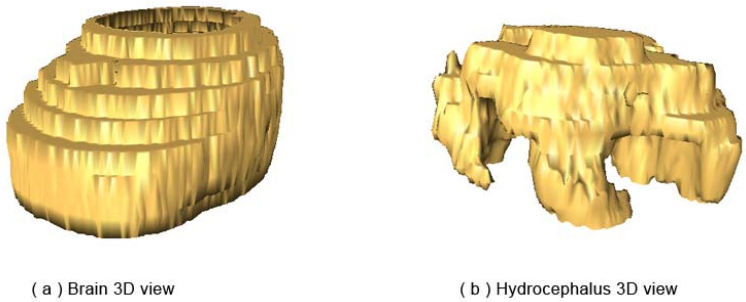

Fig. 16. Volumetric visualization of brain and hydrocephalus obtained for examination no. 1 (B ≈ 1.19 dm^3, H ≈ 0.4 dm^3, H/B = 33.67%)

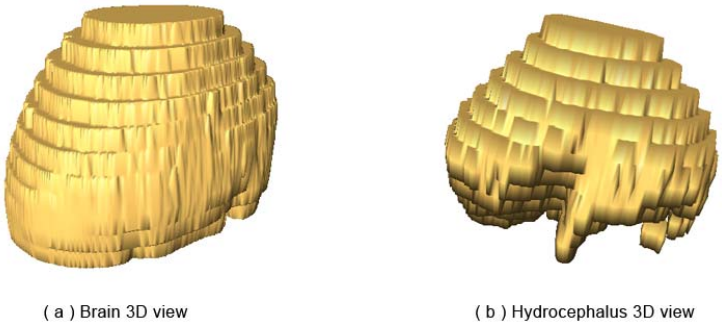

Fig. 17. Volumetric visualization of brain and hydrocephalus obtained for examination no. 4 (B ≈ 1.0 dm^3, H ≈ 0.36 dm^3, H/B = 36.5%)

Presented visualization and numerical results show, that the proposed method gives the promising results. However, it still should be remembered that precise detection of the pathological changes due to hydrocephalus is a complex problem. There are several reasons for this. Firstly, the segmentation process may be disrupted by the side effects resulting from this lesion. The disease is often accompanied by edema or hematoma of similar pixel intensity values. Because of this, segmentation results obtained by the use of the proposed methods may sometimes be inaccurate.

Furthermore, the number of the images in the dataset (and in consequence *slice thickness*) can differ significantly during next examinations. Children's

brain will also grow consequently. As a result, the calculated ratio between the volume of the hydrocephalus and the volume of the whole brain not always can be reliably compared even for the same patient.

7. CONCLUSION

In this paper problem of automation and objectification of hydrocephalus assessment based on CT and MRI brain scans was regarded. This is an important problem of recent neurosurgery as substantial methods for an automatic assessment of pathological changes due to hydrocephalus are still waiting to be developed. Moreover, popular methods for description of the disease progress are often manual or semi-manual, inaccurate and depend on subjective opinion of the radiologist.

Ideas proposed in this paper are a step forward through elimination of the abovementioned disadvantages of the traditional disease assessment methods by an application of image processing and analysis algorithms.

Preliminary results of applying the proposed algorithms to exemplary CT volumetric brain scans are promising and show that the research goes in the right direction. Intracranial space has been correctly separated from the brain using the proposed approach. The developed 2D segmentation algorithm based on region growing method with automate selection of initial seed points also gave satisfactory results on several tested cases. However, presented methods still have some imperfections. Firstly, in some cases over-segmentation appears. Additionally, the determined volumes of brain and hydrocephalus are approximate and strongly depend on spatial resolution of consecutive brain cross sections and *slice thickness* used during CT examination. Therefore, further research will be concerned on two main problems. Firstly, image segmentation algorithm will be enhanced. This will also involve improvement of the SSP algorithm, resulting in a better separation of the desired brain regions. Additionally, it is planned to develop a classifier based on fuzzy sets theory for this purpose. Next, methods for an accurate measurement of brain and hyd-rocephalus volume will be developed. This will involve reconstruction of missing information between the consecutive cross sections using data approximation techniques.

Acknowledgements

The authors would like to thank the Department of Neurosurgery of Polish Mother's Memorial Hospital – Research Institute in Lodz for providing the CT datasets used in this research.
Tomasz Węgliński is a scholarship holder of pro-ject entitled "Innovative education" supported by European Social Fund.

Anna Fabijańska receives financial support from the Foundation for Polish Science in a framework of START fellowship and from Ministry of Science and Higher Education of Poland in a framework of research project no. N N516 490439 (funds for science in years 2010-2012).

LITERATURE

1. Suetens P.: Fundamentals of Medical Imaging, Cambridge University Press, 2009.
2. Park H., Bland P.H., Meyer C.R.: Construction of an abdominal probabilistic atlas and its application in segmentation, IEEE Transactions on Medical Imaging, Vol. 22, pp. 483-492, 2003.
3. Hongkai W., Jing B., Yongxin Z., Yonghong Z.: Abdominal atlas mapping in CT and MR volume images using a normalized abdominal coordinate system, Computerized Medical Imaging and Graphics, Vol. 32, pp. 442-451, 2008.
4. van Assen H.C., Danilouchkine M.G., Frangi A.F., Ordás S., Westenberg J.J.M., Reiber J.H.C., Lelieveldt B.P.F.: SPASM: A 3D-ASM for segmentation of sparse and arbitrarily oriented cardiac MRI data, Medical Image Analysis, Vol. 10, pp. 286-303, 2006.
5. Zheng Y., Barbu A., Georgescu B., Scheuering M., Comaniciu D.: Four-chamber heart modeling and automatic segmentation for 3-D cardiac CT volumes using marginal space learning and steerable features, IEEE Transactions on Medical Imaging, Vol. 27, pp. 1668--1681, 2008.
6. Sluimer I., Schilham A., Prokop M., Van Ginneken B.: Computer analysis of computed tomography scans of the lung: A survey, IEEE Transactions on Medical Imaging, Vol. 25, pp. 385-405, 2006.
7. Fabijańska A.: Two-pass region growing algorithm for segmenting airway tree from MDCT chest scans, Computerized Medical Imaging and Graphics, Vol. 33, pp. 537-546, Elsevier, 2009.
8. Shen S., Sandham W., Granat M., Sterr A.: MRI fuzzy segmentation of brain tissue using neighborhood attraction with neural-network optimization, IEEE Transactions on Information Technology in Biomedicine, Vol. 9, pp. 459-467, 2005.
9. Stokking R., Vincken K.L., Viergever M.A.: Automatic morphology-based brain segmentation (MBRASE) from MRI-T1 data, NeuroImage, Vol. 12, pp. 726-738, 2000.
10. Prastawa M., Bullitt E., Ho S., Gerig G.: A brain tumor segmentation framework based on outlier detection, Medical Image Analysis, Vol. 8, pp. 275-283, 2004.
11. Zakrzewski K.: Wodogłowie i inne zaburzenia krążenia płynu mózgowo-rdzeniowego u dzie-ci, Czelej, Lublin, 2007 (in Polish).
12. http://www.fizyka.umk.pl/~duch/Wyklady/kog-m/new/brain-ventricles.gif, Duch W.: The Ven-tricular System of the human brain, retrieved in June 2011.
13. http://raymentspinabifida.blogspot.com/2010/07/learning-about-sb-spina-bifida-is.html, Rayments Life with Spina Bifida, retrieved in June 2011.
14. Zatz L.M.: The Evans ratio for ventricular size: A calculation error, Neuroradiology, Vol. 18, No. 2, pp. 81-81, 1979.
15. Ambarki K., Israelsson H., Wahlin A., Birgander R., Eklund A., Malm J.: Brain ventricular size in healthy elderly: comparison between Evans index and volume measurement, Neuro-surgery, Vol. 67, pp. 94–99, 2010.
16. Bradleya W.G., Safara F.G., Hurtadoa C., Orda J., Alksneb J.F.: Increased intracranial volume: A clue to the etiology of idiopathic normal-pressure hydrocephalus?, American Journal of Neuroradiology, Vol. 25, pp. 1479-1484, 2004.

17. Liu J., Huang S., Nowinski W.L.: Automatic segmentation of the human brain ventricles from MR ima-ges by knowledge-based region growing and trimming, Neuroinformatics, Vol. 7, pp. 131-146, 2009.
18. Schnack H.G., Hulshoff Pol H.E., Baaré W.F.C., Viergever M.A., Kahn R.S.: Automatic segmentation of the ventricular system from MR images of the human brain, NeuroImage, Vol. 14, pp. 95-104, 2001.
19. Hatfield F.N., Dehmeshki J.: Automatic delineation and 3-D visualisation of the human ventricular system using probabilistic neural networks, Proceedings of SPIE – The International Society for Optical Engineering, pp. 361-367, 1998.
20. Pustkova R., Kutalek F., Penhaker M., Novak V., Measurement and calculation of cerebrospinal fluid in proportion to the skull, 9th RoEduNet IEEE International Conference, RoEduNet, pp. 95-99, 2010.
21. Butman J.A., Linguraru M.G.: Assessment of ventricle volume from serial MRI scans in communicating hydrocephalus, 5th IEEE International Symposium on Biomedical Imaging: From Nano to Macro, pp. 49-52, 2008.
22. Ambarki K., Wahlin A., Birgander R., et al.: MR imaging of brain volumes: Evaluation of a fully automatic software, American Journal of Neuroradiology, Vol. 32, pp. 408-412, 2011.
23. Kobashi S., Takae T., Hata Y., Kitamura Y.T., Yanagida T., Ishikawa O., Ishikawa M.: Auto-mated segmentation of the cerebrospinal fluid and the lateral ventricles from human brain MR images, Annual Conference of the North American Fuzzy Information Processing Society – NAFIPS, pp. 1961-1966, 2001.
24. Sweetman B., Xenos M., Zitella L., Linninger A.A.: Three-dimensional computational prediction of cerebrospinal fluid flow in the human brain, Computers in Biology and Medicine, Vol. 41, pp. 67-75, 2011.
25. Halberstadt W., Douglas T.S.: Fuzzy clustering of CT images for the measurement of hydrocephalus associated with tuberculous meningitis, Annual International Conference of the IEEE Engineering in Medicine and Biology – Proceedings, pp. 4014-4016, 2005.
26. http://medical.nema.org/dicom/2004.html, Digital Imaging and Communications in Medicine, retrieved in June 2011.
27. Ridler T.W., Calvard S.: Picture thresholding using an iterative slection method, IEEE Transactions on Systems, Man and Cybernetics SMC-8 (8), pp. 630-632, 1978.
28. Tsai W.-H.: Moment-preserving thresholding: a new approach, Computer Vision, Graphics & Image Processing, Vol. 29, pp. 377-393, 1985.
29. Kapur J.N., Sahoo P.K., Wong A.K.C.: A new method for gray-level picture thresholding using the entropy of the histogram, Computer Vision, Graphics & Image Processing, Vol. 29, pp. 273-285, 1985.
30. Węgliński T., Fabijańska A.: Image segmentation algorithms for diagnosis support of hydro-cephalus in children, Automatyka, Vol. 15, No. 3, 2011 (in print).
31. Simon M.K: Probability Distributions Involving Gaussian Random Variables: A Handbook for Engineers and Scientists, Springer, 2006.

Manuscript submitted 04.07.2011

ALGORYTMY PRZETWARZANIA OBRAZÓW DLA POTRZEB OCENY I DIAGNOZY WODOGŁOWIA U DZIECI

Tomasz WĘGLIŃSKI, Anna FABIJAŃSKA

STRESZCZENIE *W niniejszym artykule przedstawiono koncepcję wykorzystania algorytmów przetwarzania i analizy obrazów do automatycznej oceny i diagnostyki wodogłowia u dzieci. Inspiracją do badań była potrzeba stworzenia skutecznych narzędzi do automatycznej (lub co najmniej półautomatycznej) detekcji i ilościowej oceny tego schorzenia dla potrzeb współczesnej neurochirurgii.*

Artykuł zawiera opis opracowanych algorytmów segmentacji obszaru wodogłowia oraz całego mózgu metodą rozrostu obszaru, a także przedstawia algorytm obliczający stosunek objętości zmiany chorobowejdo objętości całego mózgu. Niniejszy artykuł prezentuje rezultaty zastosowania proponowanych algorytmów do rzeczywistych danych obrazowych pochodzących z tomografu komputerowego. Analiza otrzymanych rezultatów pokazuje, że proponowane algorytmy mogą stanowić użyteczne narzędzie diagnostyczne do detekcji i oceny wodogłowia u dzieci.

Tomasz WĘGLIŃSKI is a PhD student at Computer Engineering Department of Technical University of Lodz (Poland). He received his MSc in Computer Science from Technical University of Lodz in 2010. His research interests focus on development of image processing and analysis algorithms for biomedical vision systems.

Anna FABIJAŃSKA is an Assistant Professor at Computer Engineering Department of Technical University of Lodz (Poland). She received her Ph.D. in Computer Science from Technical University of Lodz in 2007. Her research interests focus on development of image processing and analysis algorithms for industrial and biomedical vision systems.